Electronic Supplementary Information for:

Strong direct exchange coupling and single-molecule magnetism in indigo-bridged lanthanide dimers

Fu-Sheng Guo[a] and Richard A. Layfield*[a]

[a] School of Chemistry, The University of Manchester, Oxford Road, Manchester, M13 9PL, U.K.
E-mail: Richard.Layfield@manchester.ac.uk

General considerations

All manipulations were performed under an atmosphere of dry, oxygen-free argon, using either standard Schlenk techniques or an argon-filled glove box. All solvents were stored over activated 4 Å molecular sieves or a potassium mirror and freeze-thaw degassed prior to use. $[Cp^*_2Ln(C_3H_5)]$ (Ln = Gd, Dy)[1] and potassium graphite[2] were prepared according to literature procedures. Elemental analyses (C, H, N) were carried out at London Metropolitan University, U.K. Infrared spectra were recorded in an inert atmosphere using a Bruker Alpha FT-IR spectrometer.

$[Gd_2(Cp^*)_4(Indigo)]$, $\mathbf{1_{Gd}}$. Indigo (52 mg, 0.2 mmol) and $[Cp^*_2Gd(C_3H_5)]$ (0.188 g, 0.4 mmol) were dissolved in THF (2 ml). An immediate color change to dark red was observed. The solution was left to stand at room temperature for three days. $\mathbf{1_{Gd}}$ (0.100 g, 45%) was obtained as black needle crystals suitable for X-ray crystallography. The crystals were collected by washing with minimum amount of cold THF. Elemental analysis found (calc.)%: C: 60.35 (60.29); H: 6.10 (6.14); N: 2.53 (2.51). IR spectra (cm^{-1}, see Figure S1): 2900w, 2852w, 1603w, 1523s, 1474m, 1437s, 1377w, 1322m, 1302m, 1256s, 1222m, 1184s, 1148m, 1100w, 1054s, 1003s, 749s, 723s, 704s, 585s, 565s, 439s.

$[Dy_2(Cp^*)_4(Indigo)]$, $\mathbf{1_{Dy}}$. The synthesis of $\mathbf{1_{Dy}}$ was accomplished using the procedure described for $\mathbf{1_{Gd}}$ using $[Cp^*_2Dy(C_3H_5)]$ (0.188 g, 0.4 mmol). $\mathbf{1_{Dy}}$ was isolated as black needle crystals (0.090 g, 40%). Elemental analysis found (calc.)%: C: 59.81 (59.73); H: 6.03 (6.09); N: 2.52 (2.49). IR spectra (cm^{-1}, see Figure S2): 2901w, 2853w, 1604w, 1525s, 1476m, 1437s, 1377w, 1323m, 1303m, 1256s, 1222m, 1185s, 1148m, 1100w, 1057s, 1003s, 750s, 724s, 705s, 587s, 566s, 441s.

$[K(THF)_6][Gd_2(Cp^*)_4(Indigo)]\cdot THF$, $\mathbf{2_{Gd}}$. Indigo (52 mg, 0.2 mmol) and $[Cp^*_2Gd(C_3H_5)]$ (0.188 g, 0.4 mmol) were dissolved in THF (4 ml) and the resulting dark red solution was refluxed for 2 hours. The reaction was cooled to room temperature, and then potassium graphite (0.014 g, 0.1 mmol) was added. The reaction was filtered and the deep red filtrate was concentrated and stored at –40°C for two days. Complex $\mathbf{2_{Gd}}$ (0.084 g, 25%) was obtained as black red block crystals suitable for X-ray crystallography. The crystals were collected by washing with minimum amount of cold THF. Elemental analysis found (calc.)%: C: 60.1 (60.8); H: 7.48 (7.53); N: 1.72 (1.69). IR spectra (cm^{-1}, see Figure S3): 2853w, 1472w, 1434s, 1375w, 1329m, 1279m, 1222w, 1144m, 1064s, 1001m, 888m, 734s, 676w, 592m, 567s, 440w.

$[K(THF)_6][Dy_2(Cp^*)_4(Indigo)]\cdot THF$, $\mathbf{2_{Dy}}$. The synthesis of $\mathbf{2_{Dy}}$ was accomplished using the procedure described above for $\mathbf{2_{Gd}}$ using $[Cp^*_2Dy(C_3H_5)]$ (0.188 g, 0.4 mmol). $\mathbf{2_{Dy}}$ was isolated as dark red block crystals (0.086 g, 25%). Elemental analysis found (calc.)%: C: 60.32(60.41); H: 7.41(7.48); N: 1.69(1.68). IR spectra (cm^{-1}, see Figure S4): 2851w, 1473w, 1434s, 1374w, 1329m, 1276m, 1222w, 1144m, 1063s, 1001m, 888w, 735s, 677w, 593m, 567s, 442w.

$[K_2(THF)_5Gd_2(Cp^*)_4(Indigo)]$, $\mathbf{3_{Gd}}$. Indigo (52 mg, 0.2 mmol) and $[Cp^*_2Gd(Allyl)]$ (0.188 g, 0.4 mmol) were dissolved in 4 mL of THF and the resulting dark red solution was refluxed for 2 hours. The reaction was cooled to room temperature, and then potassium graphite (0.054 g, 0.4 mmol) was added. The

reaction was filtered and the red filtrate was concentrated and stored at –40 °C for two days. Complex $\mathbf{3_{Gd}}$ (0.187 g, 60%) was obtained as red needle crystals suitable for X-ray crystallography. The crystals were collected by washing with minimum amount of cold THF. Elemental analysis found (calc.)%: C: 58.59 (58.73); H: 7.03 (7.00); N: 1.84 (1.80). IR spectra (cm^{-1}, see Figure S5): 2846m, 1556w, 1483s, 1407s, 1337s, 1298m, 1227w, 1134s, 1085m, 1048s, 995m, 892m, 776w, 737s, 658w, 609s, 570w, 538w, 446w.

$[K_2(THF)_5Dy_2(Cp^*)_4(Indigo)]$, $\mathbf{3_{Dy}}$. The synthesis of $\mathbf{3_{Dy}}$ was accomplished using the procedure described above for $\mathbf{3_{Gd}}$ using [Cp^*_2Dy(Allyl)] (0.188 g, 0.4 mmol). $\mathbf{3_{Dy}}$ was isolated as red needle crystals (0.172 g, 55%). Elemental analysis found (calc.)%: C: 58.21(58.33); H: 6.91(6.96); N: 1.82(1.79). IR spectra (cm^{-1}, see Figure S6): 2847m, 1557w, 1484s, 1409s, 1338s, 1297m, 1228w, 1135s, 1085m, 1048s, 995m, 891m, 779w, 737s, 659w, 610s, 571w, 536w, 446w.

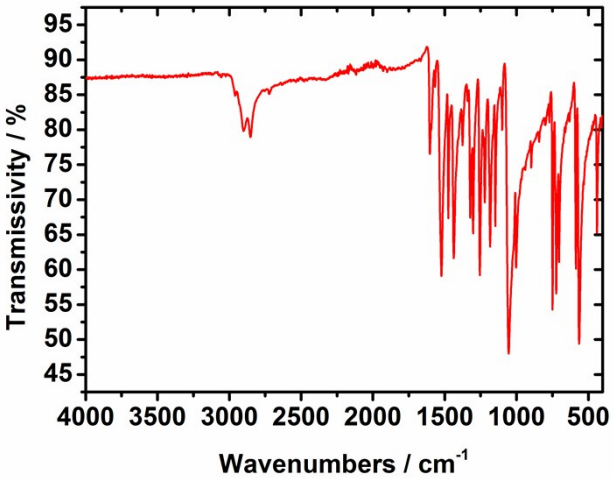

Figure S1. Infrared spectra of complex $\mathbf{1_{Gd}}$.

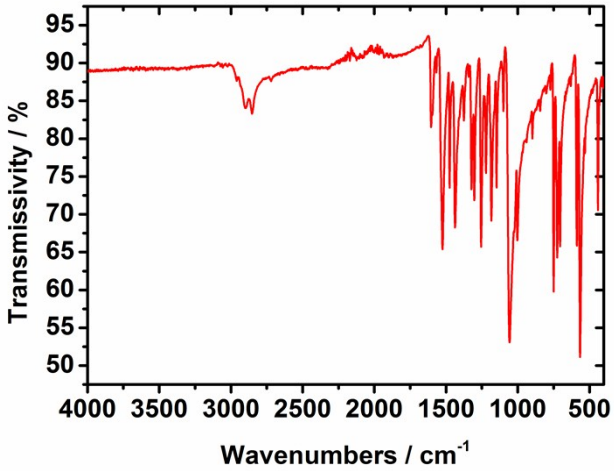

Figure S2. Infrared spectra of complex $\mathbf{1_{Dy}}$.

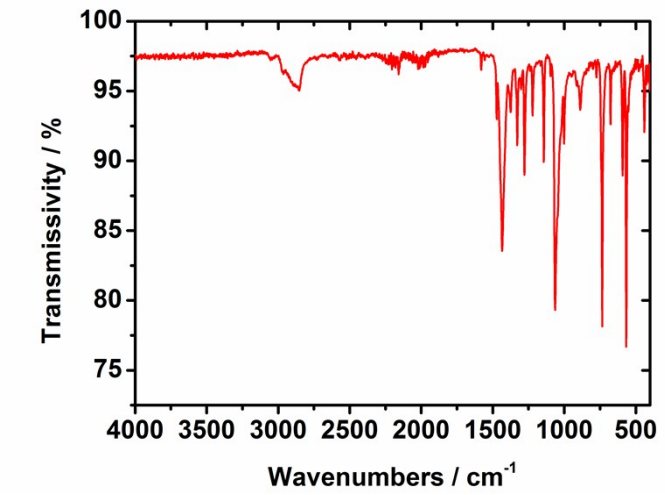

Figure S3. Infrared spectra of complex $\mathbf{2_{Gd}}$.

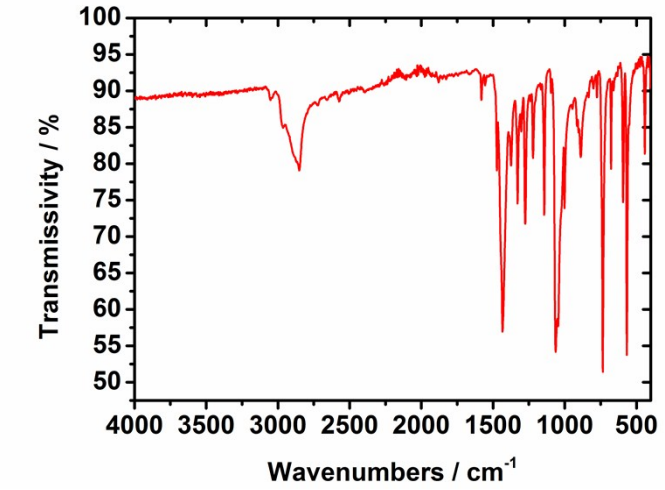

Figure S4. Infrared spectra of complex $\mathbf{2_{Dy}}$.

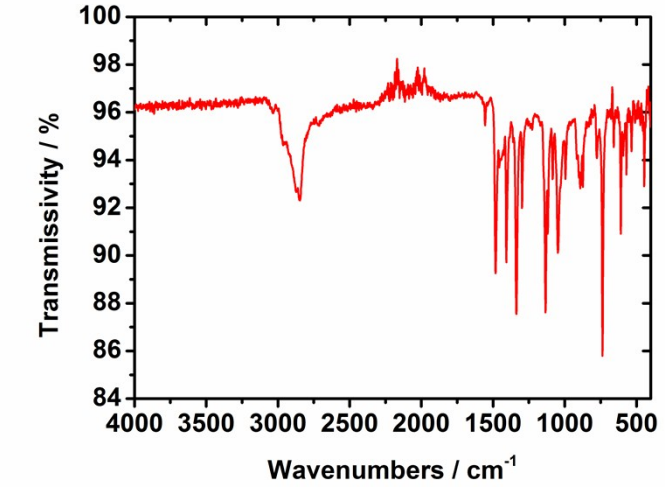

Figure S5. Infrared spectra of complex $\mathbf{3_{Gd}}$.

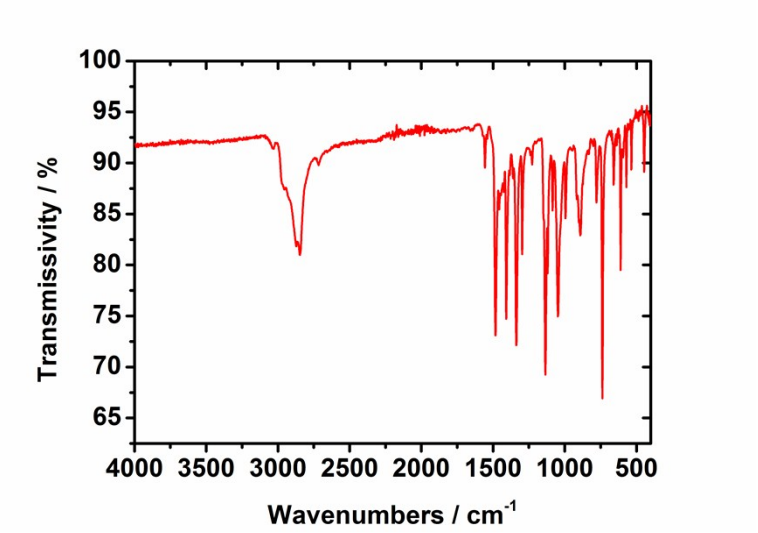

Figure S6. Infrared spectra of complex $\mathbf{3_{Dy}}$.

X-ray Crystallography

Single-crystal X-ray diffraction measurements for complexes $\mathbf{1_{Ln}}$-$\mathbf{3_{Ln}}$ were carried out on an Agilent SuperNova diffractometer with graphite monochromated MoKα radiation (λ = 0.71073 Å) at 150 K. The structures were solved by the direct method (SHELXS) and refined by full-matrix least-squares (SHELXL) on F^2.[3] Anisotropic thermal parameters were used for the non-hydrogen atoms and isotropic parameters for the hydrogen atoms. Hydrogen atoms were added geometrically and refined using a riding model. Crystallographic data and refinement details are given in Table S1.

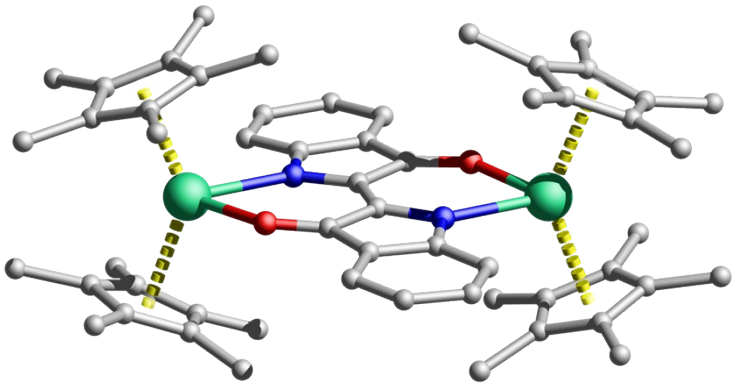

Figure S7. Structure of $\mathbf{1_{Gd}}$.

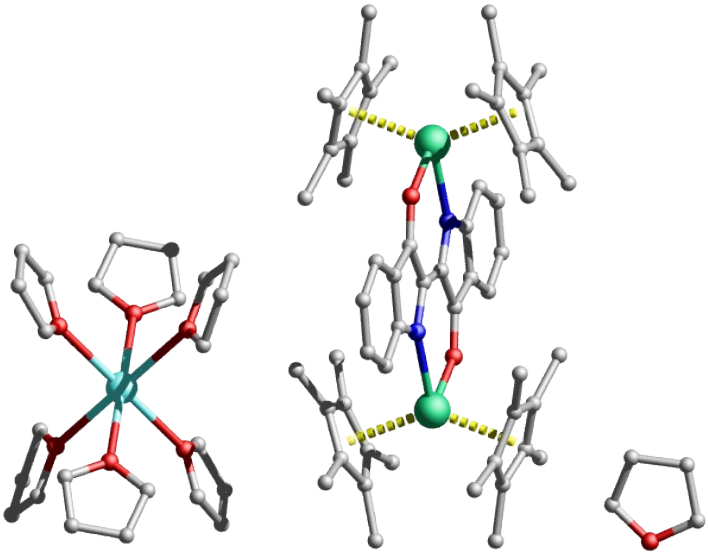

Figure S8. $[K(thf)_6][\mathbf{2_{Ln}}]\cdot thf$.

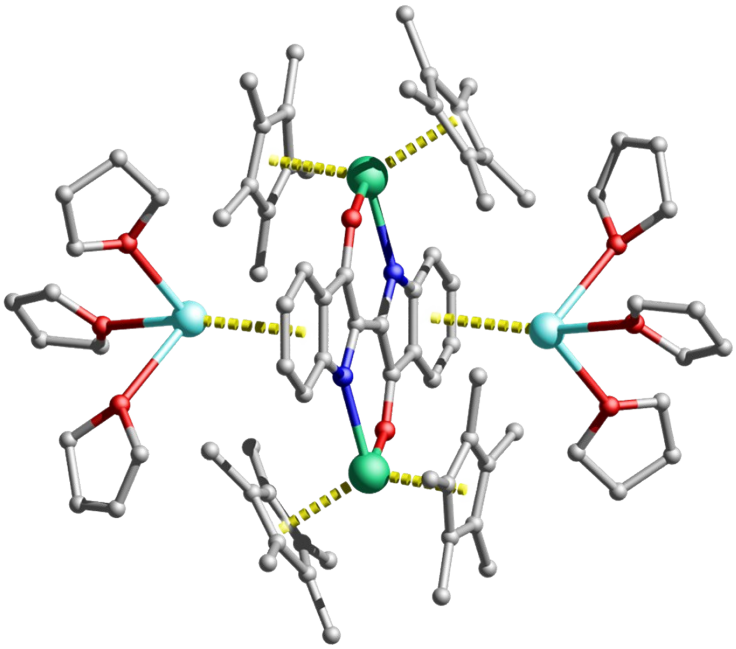

Figure S9. $[\{K(thf)_3\}_2(\mathbf{3_{Ln}})]$.

Table S1. Crystal Data and Structure Refinement for $\mathbf{1_{Ln}}$-$\mathbf{3_{Ln}}$.

Compound reference	$\mathbf{1_{Gd}}$	$\mathbf{1_{Dy}}$	$\mathbf{2_{Gd}}$	$\mathbf{2_{Dy}}$	$\mathbf{3_{Gd}}$	$\mathbf{3_{Dy}}$
Chemical formula	$C_{56}H_{68}Gd_2N_2O_2$	$C_{56}H_{68}Dy_2N_2O_2$	$C_{84}H_{124}Gd_2KN_2O_9$	$C_{84}H_{124}Dy_2KN_2O_9$	$C_{76}H_{108}Gd_2K_2N_2O_7$	$C_{76}H_{108}Dy_2K_2N_2O_7$
Formula Mass	1115.62	1126.12	1659.44	1669.94	1554.34	1564.84
Crystal system	Monoclinic	Monoclinic	Triclinic	Triclinic	Monoclinic	Monoclinic
Space group	$P2_1/c$	$P2_1/c$	P-1	P-1	$P2_1/c$	$P2_1/c$
a/Å	12.2316(3)	12.1568(3)	12.3702(4)	12.3721(5)	16.6471(13)	16.5520(13)
b/Å	20.2920(6)	20.2075(4)	13.1555(4)	13.1967(5)	11.6604(4)	11.6744(4)
c/Å	19.8739(6)	19.9643(5)	13.7622(4)	13.7762(5)	26.166(2)	25.961(2)
α/°	90	90	80.063(3)	80.217(3)	90	90
β/°	98.545(2)	98.553(2)	76.644(3)	76.392(3)	134.109(14)	133.764(14)
γ/°	90	90	81.140(3)	81.452(3)	90	90
Unit cell volume/Å^3	4878.0(2)	4849.85(19)	2131.07(12)	2140.42(14)	3646.9(8)	3622.9(7)
Temperature/K	150.01(11)	150.01(10)	150.04(13)	150.04(18)	150.03(10)	150.01(12)
No. of formula units per unit cell, Z	4	4	1	1	2	2
Radiation type	MoKα	MoKα	MoKα	MoKα	MoKα	MoKα
Absorption coefficient, μ/mm^{-1}	2.738	3.100	1.644	1.833	1.969	2.214
No. of reflections measured	20965	21399	16346	16458	15277	15624
No. of independent reflections	9562	9501	8350	8387	7156	7098
R_{int}	0.0421	0.0374	0.0236	0.0285	0.0328	0.0372
Final R_1 values ($I > 2\sigma(I)$)	0.0365	0.0333	0.0411	0.0443	0.0352	0.0365
Final $wR(F^2)$ values ($I > 2\sigma(I)$)	0.0649	0.0627	0.1077	0.1205	0.0673	0.0732
Final R_1 values (all data)	0.0564	0.0456	0.0530	0.0563	0.0458	0.0492
Final $wR(F^2)$ values (all data)	0.0724	0.0689	0.1200	0.1386	0.0743	0.0802
Goodness of fit on F^2	1.010	1.042	1.101	1.133	1.054	1.037
CCDC	1531466	1531467	1531468	1531469	1531470	1531471

$R_1 = \sum||F_o|-|F_c||/\sum|F_o|$, $wR_2 = [\sum w(F_o^2-F_c^2)^2/\sum w(F_o^2)^2]^{1/2}$

Magnetic property measurements

Magnetic measurements were recorded on a Quantum Design MPMS-XL SQUID magnetometer equipped with a 7 T magnet. Magnetic susceptibility was measured in a field of 10000 Oe in the temperature range of 2-300 K, and the frequency-dependent A.C. susceptibility was measured with an oscillating field of 1.55 Oe. Finely ground microcrystalline powder of $\mathbf{1_{Ln}}$-$\mathbf{3_{Ln}}$ was immobilized in eicosane matrix inside a flame-sealed NMR tube.

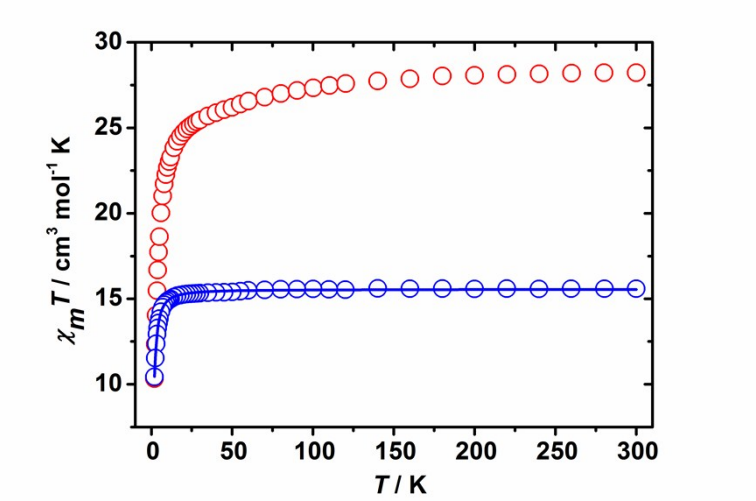

Figure S10. Plots of $\chi_M T$ versus T for $\mathbf{3_{Gd}}$ and $\mathbf{3_{Dy}}$ in an applied magnetic field of 10 kOe.

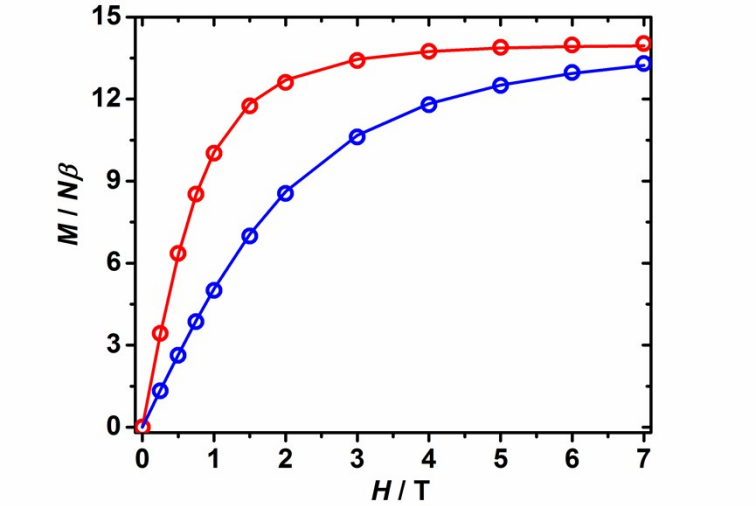

Figure S11. Field dependence of the magnetization, *M*, at 1.8 (red circles) and 5 (blue circles) K for $\mathbf{1_{Gd}}$. The solid lines are the fit to the data.

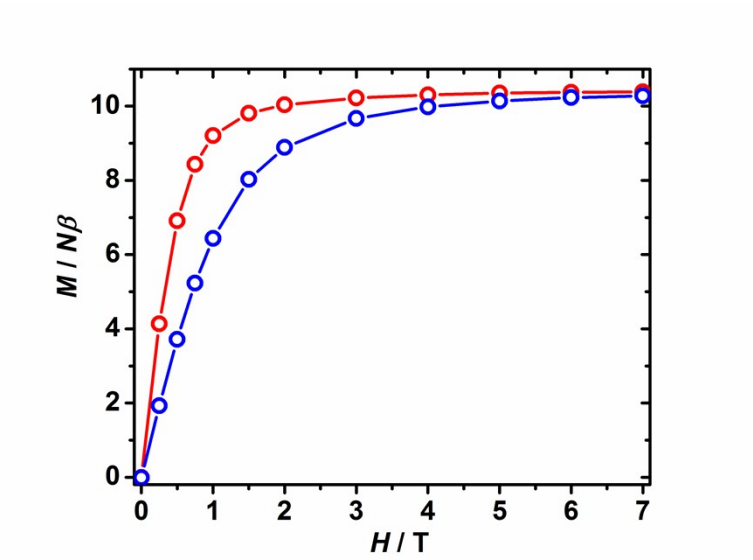

Figure S12. Field dependence of the magnetization, *M*, at 1.8 (red circles) and 5 (blue circles) K for complex $\mathbf{1}_{\mathbf{Dy}}$. The solid lines are a guide for the eye.

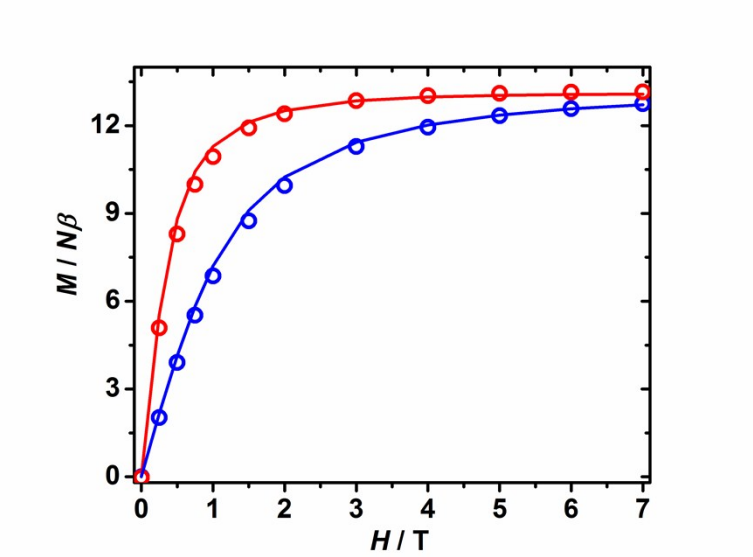

Figure S13. Field dependence of the magnetization, *M*, at 1.8 (red circles) and 5 (blue circles) K for complex $\mathbf{2}_{\mathbf{Gd}}$. The solid lines are fits to the data.

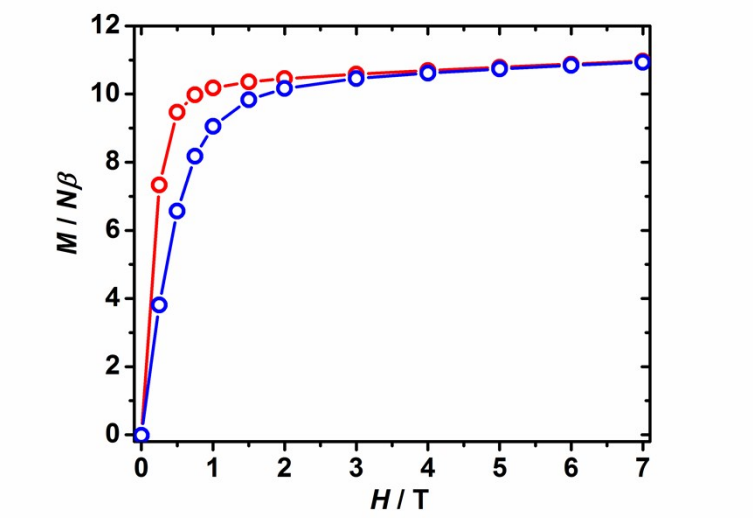

Figure S14. Field dependence of the magnetization, *M*, at 1.8 (red circles) and 5 (blue circles) K for complex $\mathbf{2}_{\mathbf{Dy}}$. The solid lines are a guide for the eye.

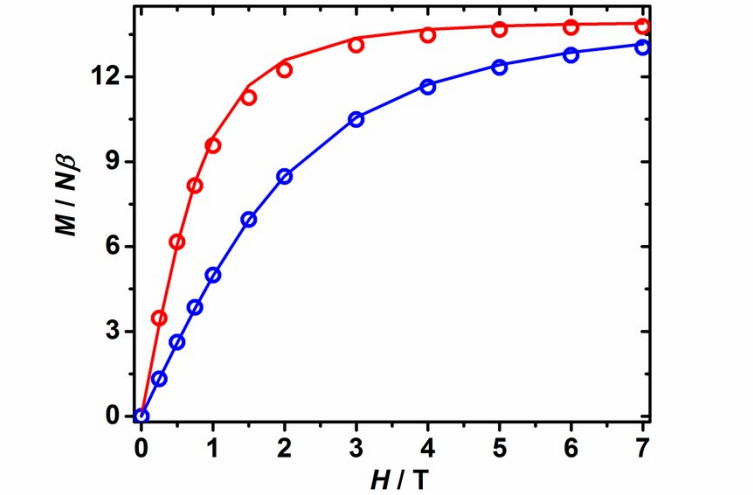

Figure S15. Field dependence of the magnetization, *M*, at 1.8 (red circles) and 5 (blue circles) K for complex $\mathbf{3}_{\mathbf{Gd}}$. The solid lines are fits to the data.

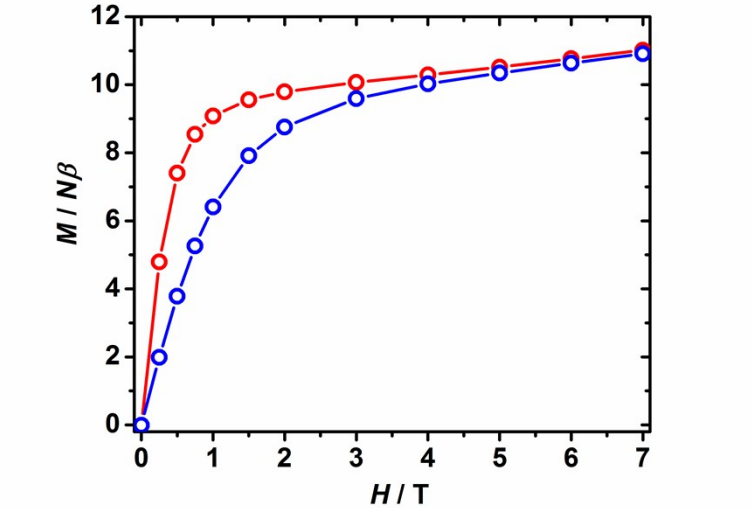

Figure S16. Field dependence of the magnetization, *M*, at 1.8 (red circles) and 5 (blue circles) K for complex $\mathbf{3}_{\mathbf{Dy}}$. The lines are the guides to the eyes.

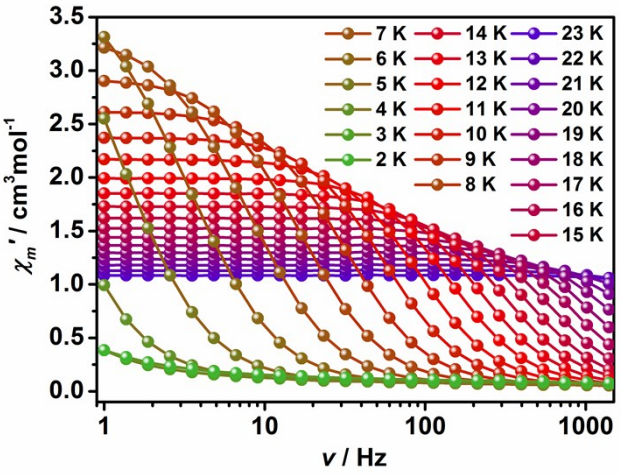

Figure S17. Frequency dependence in zero dc field of the in-phase (χ') ac susceptibility component at different temperatures for $\mathbf{1}_{\mathbf{Dv}}$.

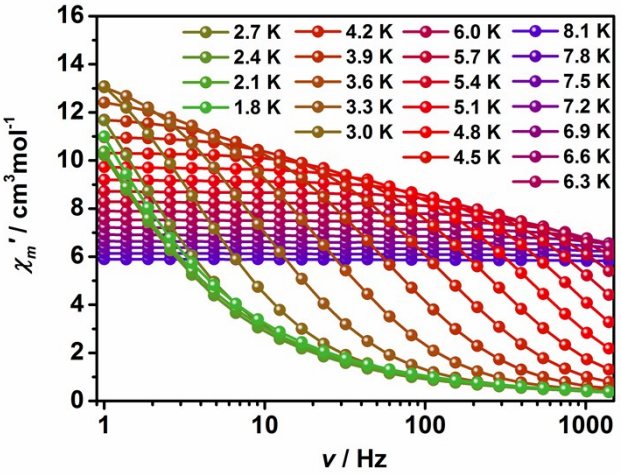

Figure S18. Frequency dependence in zero dc field of the in-phase (χ') ac susceptibility component at different temperatures for $\mathbf{2}_{\mathbf{Dv}}$.

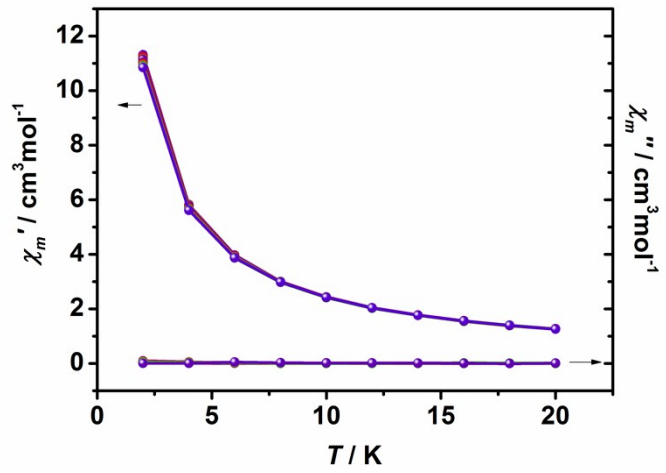

Figure S19. Temperature dependence of the in-phase (χ') and the out-of-phase (χ'') ac susceptibility component at different frequencies for $\mathbf{3}_{\mathbf{Dy}}$ (H_{dc}=0 Oe).

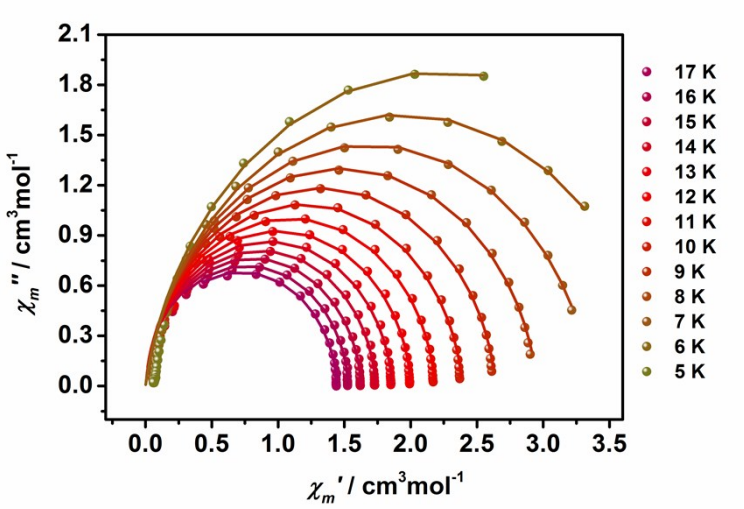

Figure S20. Cole-Cole plot using the ac susceptibility data for $\mathbf{1_{Dy}}$. The solid lines are the best fit obtained with a generalized Debye model.

Table S2. Relaxation fitting parameters from Least-Squares Fitting of $\chi(f)$ data under zero dc field of complex $\mathbf{1_{Dy}}$.

T / K	τ / s	α
17	6.50087E-5	0.02379
16	9.36023E-5	0.02554
15	1.30471E-4	0.03268
14	1.81141E-4	0.03539
13	2.51622E-4	0.03808
12	3.52686E-4	0.03895
11	4.98873E-4	0.04302
10	7.2135E-4	0.04558
9	0.00107	0.04789
8	0.00171	0.05265
7	0.00282	0.05974
6	0.00497	0.06868
5	0.0095	0.08105

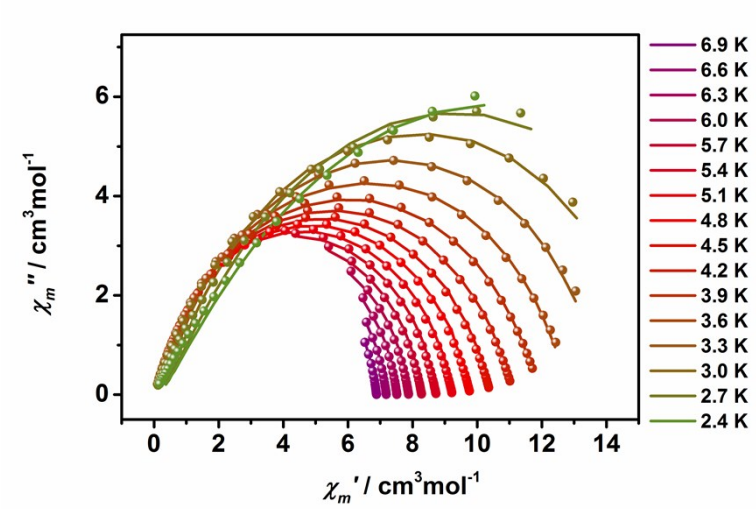

Figure S21. Cole-Cole plot using the ac susceptibility data for $\mathbf{2_{Dy}}$. The solid lines are the best fit obtained with a generalized Debye model.

Table S3. Relaxation fitting parameters from Least-Squares Fitting of $\chi(f)$ data under zero dc field of complex $\mathbf{2_{Dy}}$.

Temperature / K	τ / s	α
6.9	8.04972E-6	0.11053
6.6	1.11272E-5	0.10781
6.3	1.53902E-5	0.1095
6.0	2.21458E-5	0.11534
5.7	3.16844E-5	0.12877
5.4	4.62094E-5	0.1488
5.1	7.05213E-5	0.16799
4.8	1.13182E-4	0.18505
4.5	1.90648E-4	0.20251
4.2	3.42079E-4	0.21815
3.9	6.55879E-4	0.23141
3.6	0.00134	0.24281
3.3	0.00293	0.25096
3.0	0.0068	0.25433
2.7	0.01652	0.26048
2.4	0.04225	0.28519

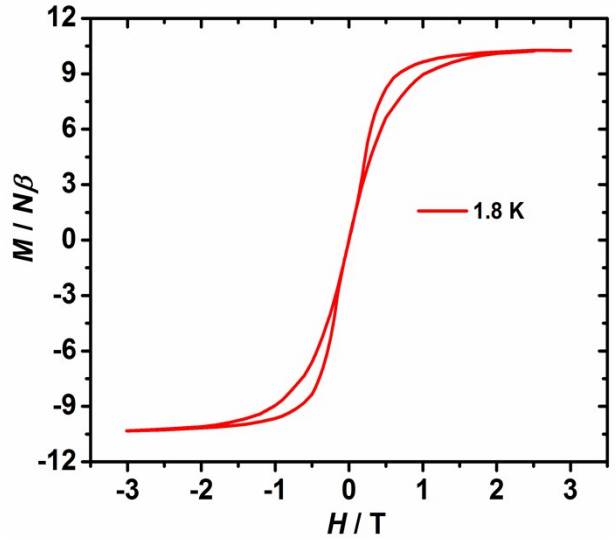

Figure S22. The hysteresis loop for $\mathbf{1}_{Dy}$ using an average field sweep rate of 2.1 mT s^{-1} at 1.8 K.

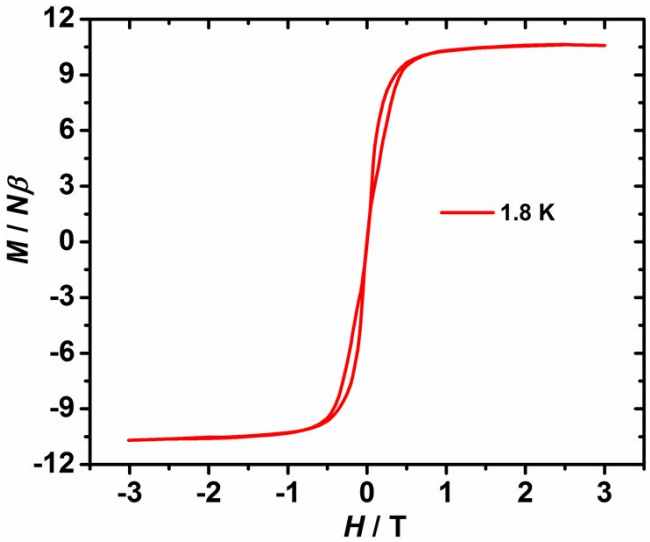

Figure S23. The hysteresis loop for $\mathbf{2}_{Dy}$ using an average field sweep rate of 2.1 mT s^{-1} at 1.8 K.

1. S. Demir, J. M. Zadrozny, M. Nippe and J. R. Long, *J. Am. Chem. Soc.*, 2012, **134**, 18546.
2. W. J. Evans, S. A. Kozimor, J. W. Ziller, N. Kaltsoyannis, *J. Am. Chem. Soc.,* 2004, **126**, 14533.
3. (a) G. M. Sheldrick, SHELXS-2014, Program for Crystal Structure Solution, University of Göttingen, 2014; (b) G. M. Sheldrick, *Acta Cryst. A*, 2008, **64**, 112.